$\alpha + \alpha$ scattering reexamined in the context of the São Paulo potential

L. C. Chamon,[1] B. V. Carlson,[2] and L. R. Gasques[1]

[1]Departamento de Física Nuclear, Instituto de Física da Universidade de São Paulo, Caixa Postal 66318, 05315-970, São Paulo, SP, Brazil

[2]Departamento de Física, Instituto Tecnológico de Aeronáutica, Centro Técnico Aeroespacial, São José dos Campos, SP, Brazil

(Received 3 January 2011; revised manuscript received 28 February 2011; published 29 March 2011)

We have analyzed a large set of $\alpha + \alpha$ elastic scattering data for bombarding energies ranging from 0.6 to 29.5 MeV. Because of the complete lack of open reaction channels, the optical interaction at these energies must have a vanishing imaginary part. Thus, this system is particularly important because the corresponding elastic scattering cross sections are very sensitive to the real part of the interaction. The data were analyzed in the context of the velocity-dependent São Paulo potential, which is a successful theoretical model for the description of heavy-ion reactions from sub-barrier to intermediate energies. We have verified that, even in this low-energy region, the velocity dependence of the model is quite important for describing the data of the $\alpha + \alpha$ system.

DOI: 10.1103/PhysRevC.83.034617 PACS number(s): 24.10.Ht, 25.55.Ci

I. INTRODUCTION

Heavy-ion reactions represent a quite important subject, which was extensively studied in the last decades. Because of the many degrees of freedom involved in the collision of two nuclei with complicated structure, many different channels, such as elastic and inelastic scattering, transfer reactions, and fusion processes, are coupled in the final state. Obviously, a certain degree of simplification is necessary to obtain a solution for such a complex problem. Thus, heavy-ion elastic scattering data analyses have usually been performed within the context of the optical model, where a phenomenological imaginary part of the potential simulates the absorption of flux from the elastic to the reaction channels. Another approach frequently used in data analyses is characterized by coupled-channel (CC) calculations, in which a few superficial reaction channels, mostly related to inelastic and transfer processes, are explicitly considered in the solution of the coupled equations. Even so, because of the great difficulty of describing in detail the fusion channels, CC calculations always involve an imaginary part of the interaction to simulate the fusion process. Furthermore, some degree of approximation is also present in the representation of the nuclear states adopted to calculate the coupling potentials. Therefore, data analyses for heavy-ion systems always involve approximations and assumptions in the corresponding theoretical calculations. The strong absorption at small distances of interaction, related to the large superposition of the nuclear densities, makes the theoretical elastic scattering cross-section calculations rather insensitive to the real part of the optical potential at these inner distances. Thus, the corresponding data analyses mostly probe the superficial region where the competition between the attractive nuclear and the repulsive Coulomb potentials results in a barrier.

Heavy-ion elastic scattering data have been obtained and analyzed for many systems and in a very wide energy range. For each system, the corresponding strengths of the real part of the phenomenological optical potentials, in the surface region, present significant energy dependence (for a review, see Ref. [1]). The São Paulo potential (SPP) [2] is a theoretical model for the real part of the nuclear interaction that accounts for this energy dependence. The model was widely and successfully applied in data analyses of many heavy-ion systems from sub-barrier to intermediate energies. The SPP was assumed in studies of different reaction channels such as elastic scattering for systems involving tightly bound (see e.g., [3,4]), weakly bound (e.g., [5,6]), and halo (e.g., [7,8]) nuclei; heavy-ion fusion of tightly bound (e.g. [9,10]), weakly bound, and exotic (e.g., [11,12]) nuclei; and inelastic scattering and transfer processes (e.g., [13,14]). Furthermore, because the model is based on a folding procedure, the SPP includes a systematics of nuclear densities and, therefore, possesses no adjustable parameters in the real part of the interaction. This characteristic makes the SPP an important tool for making predictions rather than simple data fits.

Elastic α-nucleus scattering processes have also been extensively studied from the theoretical and experimental perspective (e.g., [15,16]). The α-nucleus potential, generally employed to analyze elastic scattering data, is also an important ingredient in the description of many other nuclear reactions. For example, the knowledge of these potentials is crucial in calculations of α-capture and α-transfer reactions, as well as α decay of heavy nuclei, with particular application in reactions of astrophysical interest. In the last decades, there have been many attempts to obtain global α-nucleus potentials, using the double-folding formalism or Woods-Saxon parametrizations (e.g., [17–19]). Within this context, the SPP was also successfully used to describe α-nucleus elastic scattering data and fusion cross sections in a wide range of energies (e.g., [3,11,20]).

There are many available elastic scattering data for the $\alpha + \alpha$ system, for which reaction channels are negligible at low bombarding energies. In fact, the first ^{4}He excited state has a high excitation energy of 20.1 MeV. For bombarding energies below 34.6 MeV, the compound nucleus, ^{8}Be, must decay into two alphas, because the threshold for the first particle channel, ^{7}Li + p, lies at $Q = 17.3$ MeV. Thus, the only open reaction channel at low bombarding energies corresponds to the ^{4}He(^{4}He,γ)^{8}Be process, which is related to the 0^+ (ground state), 2^+ (excitation energy of about 3 MeV), and 4^+ (excitation energy of about 11.4 MeV) ^{8}Be states. Even so, theoretical (see e.g., [21–23]) and experimental [24] works indicate very low cross sections (about 150 nb or less) for these processes. Therefore, owing to the lack of open reaction channels, the optical model analyses of the $\alpha + \alpha$ elastic data must be realized without an imaginary part in the optical potential. This important characteristic allows one to probe the real part of the potential at quite small interaction distances. Another interesting point of the $\alpha + \alpha$ system is the rather small number of partial waves involved in the scattering at low energies, further reduced to only even values because of the identical character of the particles. This allows the determination of the corresponding (real) phase shifts almost without ambiguities from the data. For a long time, it was believed that the experimental phase shifts could be described only if the nuclear potential depended strongly on the angular momentum (for review, see [25,26]). In 1977, Buck, Friedrich and Wheatley obtained a potential (hereafter labeled as BFWP) [27] which has a Gaussian shape and is independent of both energy and angular momentum. By adjusting two parameters of the Gaussian, they obtained a quite good description of the $\alpha + \alpha$ phase shifts and also a good description of the position and width of the resonance corresponding to the ^{8}Be ground state. Beyond the simple two-body approach, there are other classes of studies that treat the α-α interaction as a system containing eight nucleons and ruled by the basic two-nucleon force. Examples of these models are the generator coordinate method (GCM) and the resonating group formalism (RGF) (e.g., [26]). Indeed, a study of the breakup of the ^{8}Be into two alphas in the context of the GCM shown that the corresponding α-α interaction is compatible with the SPP (see Fig. 4 of Ref. [28]).

Taking all these characteristics into account, the main purpose of the present paper is to investigate the accuracy and possible limitations with which the SPP, a model that was so successful in the description of α-nucleus and heavy-ion systems, can also describe the $\alpha + \alpha$ elastic data. This goal represents a challenge and a further test of the SPP because, as we have already discussed, heavy-ion data mostly probe the surface region of the interaction while the $\alpha + \alpha$ elastic data is sensitive also to the inner region. We show that the velocity dependence of the SPP, which was established by comparing heavy-ion data analyses at low and high energies [29], is also important in the description of the low energy $\alpha + \alpha$ data. The present work should open a door to extending the SPP model to the study of systems involving light nuclei.

II. THE SÃO PAULO POTENTIAL

In the context of the SPP, the interaction is more appropriately described in terms of a velocity dependence, which arises from the Pauli nonlocality [2,29], rather than an energy dependence. The SPP can be expressed in two equivalent versions [2]:

$$V_N(R) = V_0 \int \rho_{1m}(\vec{r}_1)\rho_{2m}(\vec{r}_2)\delta(\vec{R} - \vec{r}_1 + \vec{r}_2)\, e^{-4\mathrm{v}^2/c^2}\, d\vec{r}_1\, d\vec{r}_2, \quad (1)$$

$$V_N(R) = \int \rho_1(\vec{r}_1)\rho_2(\vec{r}_2)v_{nn}(\vec{R} - \vec{r}_1 + \vec{r}_2)\, e^{-4\mathrm{v}^2/c^2}\, d\vec{r}_1\, d\vec{r}_2, \quad (2)$$

where $V_0 = -456$ MeV fm^3. Equation (1) represents the zero-range approach, characterized by the Dirac delta associated with the matter distributions of the nuclei, while Eq. (2) involves a finite range effective nucleon-nucleon interaction associated with the nucleon densities of the nuclei. The matter distribution differs from the nucleon density because of the finite size of the nucleon [2]. In Eqs. (1) and (2), c is the speed of light and v represents the local relative velocity between the two nuclei, which is related to the kinetic energy by

$$K = \frac{\mu c^2}{\sqrt{1 - \mathrm{v}^2/c^2}} - \mu c^2 = E_{\mathrm{c.m.}} - V_N(R) - V_C(R), \quad (3)$$

where μ is the reduced mass of the system, $E_{\mathrm{c.m.}}$ is the bombarding energy in the center-of-mass frame, and $V_C(R)$ is the Coulomb potential. In the present case, we also calculate $V_C(R)$ using a folding procedure with the ^{4}He charge distribution obtained from electron scattering experiments [30]. The model was applied to data analyses for energies ranging from sub-barrier up to 200 MeV/nucleon ($v \approx 0.57\, c$).

The behavior of the volume integrals (J_R) of the real part of the interaction, extracted from the data analyses of many systems, including those involving light nuclei, indicates that the SPP model should be appropriate at even higher velocities ($v \approx 0.7\, c$) [32]. In particular, α-nucleus volume integrals that have been obtained through different models are compatible with the corresponding SPP predictions. For instance, data analyses for α + ^{90}Zr at $E_{\mathrm{Lab}} = 15$ MeV have resulted in $J_R = 300$ [17], 337 [18], and 443 [15] MeV fm^3 which should be compared with the SPP result of 360 MeV fm^3. Also for α + ^{208}Pb at $E_{\mathrm{Lab}} = 27$ MeV, the values $J_R = 336$ [18] and 342 [31] MeV fm^3 have been reported and the SPP provides 354 MeV fm^3.

To obtain a parameter-free interaction, Ref. [2] also includes a systematics of matter distributions and nucleon densities. Within this systematics, the SPP does not contain any adjustable parameter and, therefore, the model can be used to obtain cross-section predictions instead of simple data fits. However, the systematics for heavy ion is not appropriate for describing ^{4}He scattering. We thus assumed that the α matter and charge distributions have the same shape and, therefore, $\rho_m(r)$ in Eq. (1) is simply equal to twice the charge distribution. This approach seems quite reasonable because both the charge and matter distributions already take into account the finite size of the nucleon [2].

Considering the Pauli exclusion principle, for heavy-ion systems the assumption of frozen densities for the interaction can be criticized when dealing with very small separations, because of the large superposition of the target and projectile nuclear densities. On the other hand, because the α particle is very tightly bound with high excitation energies, the assumption of a rigid configuration should be a good approximation in the present case even at small interaction distances.

The BFWP, $V_N(R) = -U_0\, e^{-\alpha R^2}$ with $U_0 = 122.6225$ MeV and $\alpha = 0.22$ fm^{-2} [27], is represented by the solid line in Fig. 1 (top). The sum of this potential with the corresponding Coulomb interaction, $V_C(R) = 4e^2\mathrm{erf}(0.75R)/R$, is illustrated in Fig. 1 (bottom). In the energy region studied in

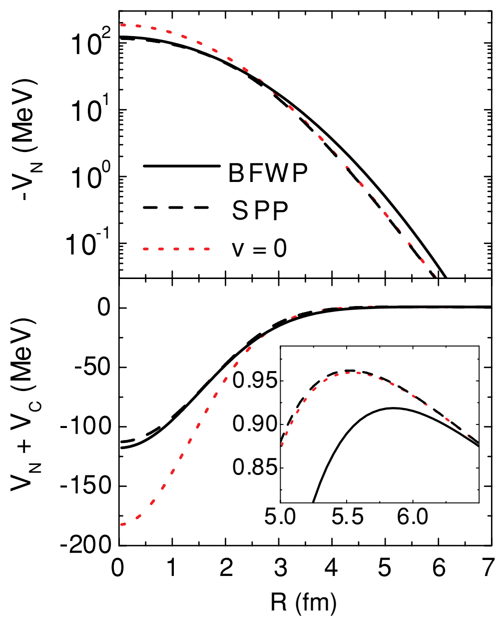

FIG. 1. (Color online) (Top) SPP (dashed line) and BFWP (solid line) for the $\alpha + \alpha$ system. To illustrate the effect of the velocity dependence of the SPP, the dotted lines in the figure correspond to Eq. (1) with $v = 0$. (Bottom) Nuclear plus corresponding Coulomb potentials as a function of the distance of interaction. The region of the s-wave barrier radius is enhanced in the inset.

the present work, the SPP does not vary significantly. Thus, we represent the SPP in Fig. 1 (dashed lines) considering an average energy of $E_{\text{Lab}} \approx 15$ MeV. The SPP is quite similar to the BFWP for $R \leqslant 3$ fm but is significantly smaller than the BFWP for larger interaction radii. Even so, both interactions provide similar barrier radii with barrier heights that differ by only about 50 keV (see inset in Fig. 1). Thus, it is expected that the SPP could, with a possible small renormalization, provide a good description of the elastic scattering data. With the aim of illustrating the effect of the velocity dependence of the SPP, we also show the potential obtained by assuming $v = 0$ in Eq. (1) (see dotted lines in Fig. 1). This potential differs significantly from the BFWP for all values of R and thus cannot provide a good description of the experimental phase shifts (as we shall demonstrate in Sec. IV). Therefore, the velocity dependence of the SPP is clearly very important in accounting for the experimental data of the $\alpha + \alpha$ system even at low energies. This behavior can be understood from Eqs. (1) and (3). At low energies and in the surface region, because of the vanishing nuclear interaction, the relative velocity is small ($v \approx 0.085\,c$ for $E_{\text{Lab}} \approx 15$ MeV) and therefore no significant effect of the velocity is observed in the interaction at the surface (compare dotted and dashed lines in Fig. 1). On the other hand, because of the strong nuclear potential, at smaller distances the relative velocity is large ($v \approx 0.34\,c$), resulting in a reduction of the nuclear interaction in this region (Fig. 1). The shape of the velocity-dependent SPP is thus quite different from that considering $v = 0$.

III. THE ^{8}BE GROUND STATE

When dealing with deep potentials like the BFWP, there are solutions of the Schrödinger equation with negative energy that would correspond to ^{8}Be bound states (see e.g., [27,33]). These spurious bound states are microscopically understood within the framework of the RGF as states forbidden by the Pauli principle [33]. Thus, the ground state of ^{8}Be is, in fact, unbound with an experimental Q value (relative to the two-alpha channel) of about 92 keV and a width of about 6 eV.

The BFWP gives a good description of the resonance observed in the $\alpha + \alpha$ system related to the ^{8}Be ground state. Figure 2(a) shows the behavior of $\sin^2(\delta_0)$ (δ_0 is the s-wave theoretical phase shift) as a function of the energy of the $\alpha + \alpha$ system. Our calculations with the BFWP present a resonance at $E_R \approx 177$ keV with a width of $\Gamma = 870$ eV. These values are very different from those reported in the original reference [27]. This discrepancy is not significant because E_R and Γ are quite sensitive to the numerical calculations realized to solve the Schrödinger equation, so that very small differences in values adopted for constants such as e^2, $\hbar c$, the α mass, etc., can produce quite distinct values for E_R and Γ. For the same reason, very small variations in the parameters U_0 and α of the BFWP also produce large variations in E_R and Γ, as illustrated in Figs. 2(b) and 2(c). There are several other models that study and reproduce the properties of the ^{8}Be (e.g., [22,23,34]). The standard SPP does not reproduce this resonance correctly. Thus, we have introduced a renormalization factor in V_0 of Eq. (1) through $V_0 = -N$ 456 MeV fm^3 (obviously, $N = 1$ corresponds to the standard SPP). We obtained a good description of the resonance with $N = 1.0812$ [see Fig. 2(d)] that corresponds to $V_0 \approx 493$ MeV fm^3. We discuss the possible effect of this renormalization on the results of heavy-ion systems in Sec. V.

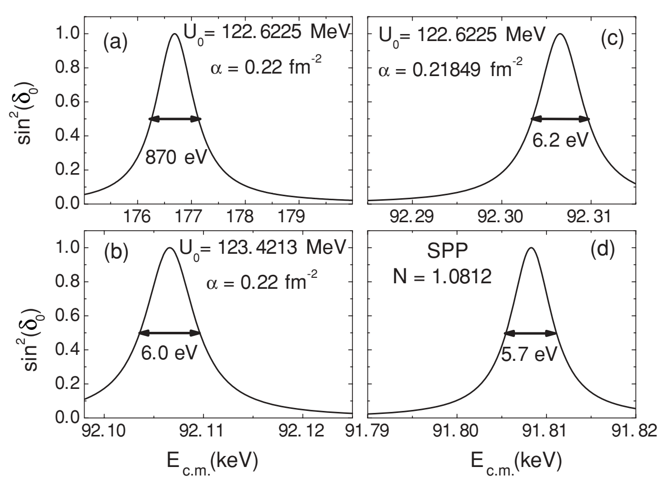

FIG. 2. Theoretical description of the resonance in the $\alpha + \alpha$ s-wave phase shift (δ_0) because of the ground state of ^{8}Be, considering the following: (a) the present calculations with the BFWP, (b) and (c) small variations of the U_0 and α parameters of the BFWP, respectively, and (d) the SPP renormalized with $N \approx 1.08$. The corresponding widths are indicated in the figure.

IV. ELASTIC SCATTERING DATA ANALYSES

We analysed 42 elastic scattering angular distributions in the energy range of $0.6 \leqslant E_{\rm Lab} \leqslant 29.5$ MeV. The data and corresponding experimental phase shifts were obtained from Refs. [35] ($2.96 \leqslant E_{\rm Lab} \leqslant 4.98$ MeV), [36] ($0.6 \leqslant E_{\rm Lab} \leqslant 3$ MeV), [37,38] ($12.3 \leqslant E_{\rm Lab} \leqslant 22.81$ MeV), [39] ($3.84 \leqslant E_{\rm Lab} \leqslant 11.88$ MeV), and [40] ($18 \leqslant E_{\rm Lab} \leqslant 29.5$ MeV). In Fig. 3(a), we illustrate the good agreement between experimental and theoretical results for phase shifts obtained with the BFWP. We point out that the phase shifts are not as sensitive to tiny variations in the potential as the parameters of the ^{8}Be resonance. We show the results for phase shifts of the SPP with $N = 1$ (dashed lines) and $N = 1.081$ (solid lines) in Fig. 3(b). In Figs. 4 and 5 the corresponding elastic scattering cross sections are presented for several angular distributions. Because of the identical character of target and projectile, the angular distributions are symmetric relative to 90°. The theoretical elastic cross sections are very sensitive to the small (about 8%) renormalization of the potential. The renormalized SPP provides a good description of the data at several energies but it clearly fails at others. Indeed, from the phase shifts shown in Fig. 3(b) it can be understood whether the corresponding experimental angular distributions can be well described or not by the theoretical calculations. For instance, at $E_{\rm Lab} \leqslant 3$ MeV the experimental s-wave phase shifts are in good agreement with those from the $N = 1.081$ theoretical calculation and larger than those obtained with $N = 1$. At $E_{\rm Lab} = 5.26$ MeV, the experimental d-wave phase shift is not described by the $N = 1$ calculation while $N = 1.081$ provides a theoretical value that approaches the experimental one. For $E_{\rm Lab} > 20$ MeV, the experimental $L = 4$ phase shifts are larger than the theoretical values for both: $N = 1$ and $N = 1.081$.

The curves of Fig. 3(b) indicate that the phase shifts for higher angular momenta could be described by considering slightly higher values of N. Thus, we performed a fit of all angular distributions taking N to be a free parameter for different L values. In this energy region, the data fits are rather insensitive to the N value assumed for $L \geqslant 6$ and, therefore, we fixed $N = 1.081$ for these angular momenta. The best fit was obtained with $N = 1.081$ for $L = 0$, $N = 1.098$ for L = 2, and $N = 1.133$ for $L = 4$ (hereafter we refer to this potential model as the L-dependent SPP). Figure 3(c) shows the corresponding phase shifts. The dashed lines in Figs. 6 and 7 illustrate the respective angular distributions. With the aim of comparison, the solid lines in Figs. 6 and 7 correspond to the results obtained with the BFWP. At low energies the results of the L-dependent SPP are almost indistinguishable from those of the BFWP (Fig. 6), but at higher energies, despite the quite reasonable agreement obtained with the SPP, the BFWP provides slightly better fits to the data (Fig. 7). We emphasize that the L dependence obtained with the SPP from the data fits is very weak. In fact, the N values vary less than 5% from $L = 0$ ($N = 1.081$) to $L = 4$ ($N = 1.133$).

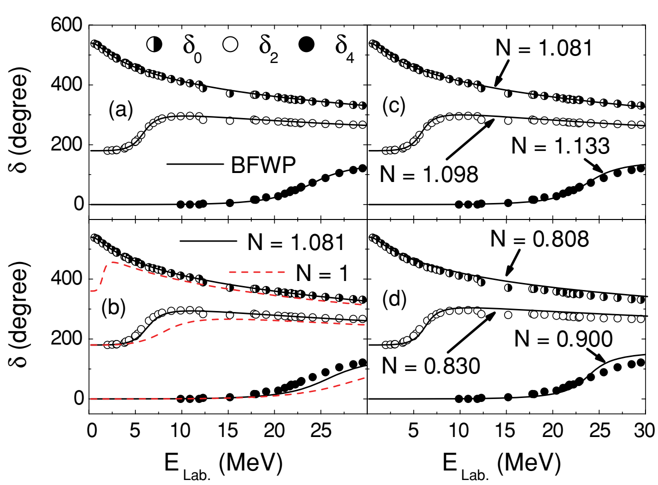

FIG. 3. (Color online) Comparison between experimental phase shifts (from Refs. [35,36,38–40]), for $L = 0$, 2, and 4, with theoretical results for (a) the BFWP, (b) the SPP with $N = 1.081$ (solid lines) and with $N = 1$ (dashed lines), (c) the L-dependent SPP, and (d) the phase shifts obtained with Eq. (1) assuming $v = 0$. The N values adopted in the calculations are indicated in the figure.

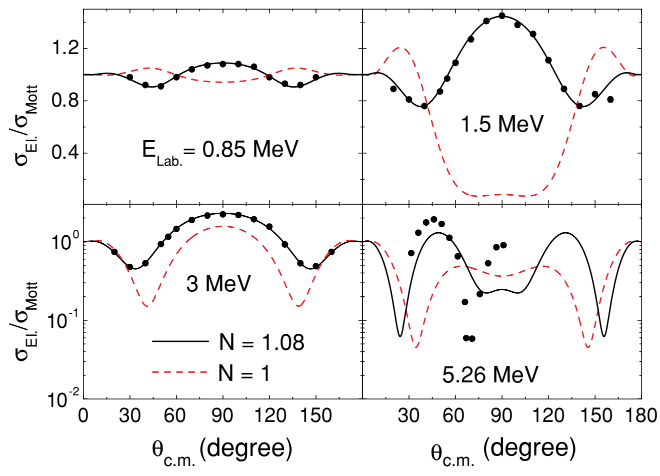

FIG. 4. (Color online) Elastic scattering data from Refs. [36,39] for $E_{\rm Lab} = 0.85$, 1.5, 3, and 5.26 MeV. The dashed and solid lines represent the theoretical results obtained with the SPP with $N = 1$ and $N = 1.081$, respectively.

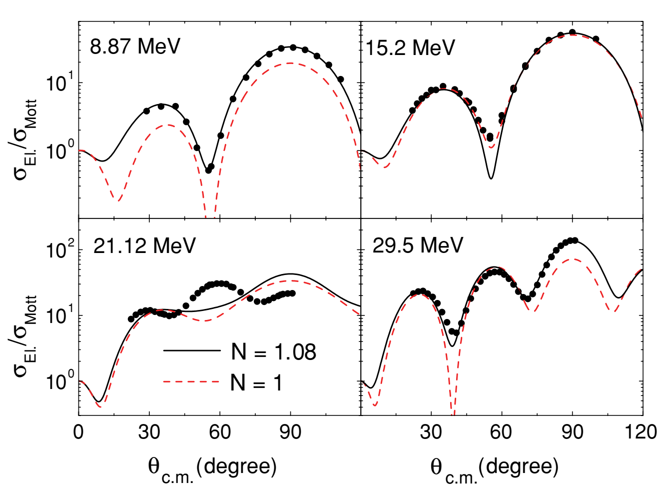

FIG. 5. (Color online) The same as Fig. 4, for $E_{\rm Lab} = 8.87$, 15.2, 21.12, and 29.5 MeV (data from Refs. [37,39,40]).

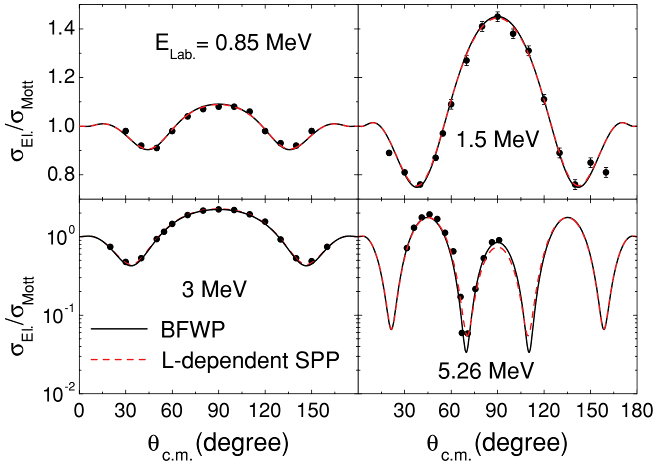

FIG. 6. (Color online) Elastic scattering data from Refs. [36,39] for $E_{\mathrm{Lab}} = 0.85$, 1.5, 3, and 5.26 MeV. The dashed and solid lines represent the theoretical results of the L-dependent SPP and BFWP, respectively. Observe that the scale for $E_{\mathrm{Lab}} = 0.85$ and 1.5 MeV is different from that of Fig. 4.

We return, now, to the importance of the velocity dependence of the SPP in describing the $\alpha + \alpha$ elastic scattering data. To illustrate this point, we have performed calculations with Eq. (1) assuming $v = 0$, but adjusting the V_0 value. In this context, it is possible to describe the ^{8}Be resonant ground state assuming $N \approx 0.808$ for $L = 0$. Nevertheless, the corresponding predictions for the s-wave phase shifts are in disagreement with the experimental values at high energies, as illustrated in Fig. 3(d). We also tried to fit the experimental phase shifts for $L = 2$ (with $N \approx 0.83$) and $L = 4$ ($N \approx 0.90$) at low energies but again the extrapolation of the theoretical values to higher energies fails to account for the data [Fig. 3(b)]. This behavior clearly indicates that the shape of the SPP without considering the velocity dependence is not appropriate to fit the data, as already discussed in Sec. II.

As an alternative approach to fitting the data in the context of the SPP, but now without any L dependence in the interaction, we have searched for a matter distribution with a shape different from that of the charge distribution. We assumed a two-parameter Fermi function to describe the α-matter distribution:

$$\rho(r) = \frac{\rho_0}{1 + e^{(r - R_0)/a}}. \tag{4}$$

In these conditions, different sets of a and R_0 parameters provide good elastic data fits, quite similar to those obtained with the BFWP, and also describe the ^{8}Be resonance. For all these sets the corresponding (L independent) N values are about 1.11. The best fit parameters correspond to $R_0 = 1.162$ fm, $a = 0.42$ fm, and $N = 1.1144$. In Fig. 8 we show that the shape of the best-fit matter distribution is rather different from that of the α charge (multiplied by two). It is worth mentioning the importance of having, within the context of the SPP, an L-independent α-α potential which provides a satisfactory description of the experimental phase shifts and properties of ^{8}Be. Prior to the work of Buck *et al.* [27], all phenomenological α-α potentials featured a dependence on the angular momentum to describe the data (see [25] and references therein).

There are thus two different approaches in which the SPP can account for the $\alpha + \alpha$ elastic scattering data. In one of these, in which the SPP is totally equivalent to the BFWP, it is necessary to assume that the matter and charge distributions have different shapes. In the other, an additional weak L dependence is applied to the interaction. L dependence is generally related to a deformed potential but the α particle is considered a spherical nucleus. What could be the possible origin of such a deformation? We believe that the deformation might arise from effects of relativistic contraction of space.

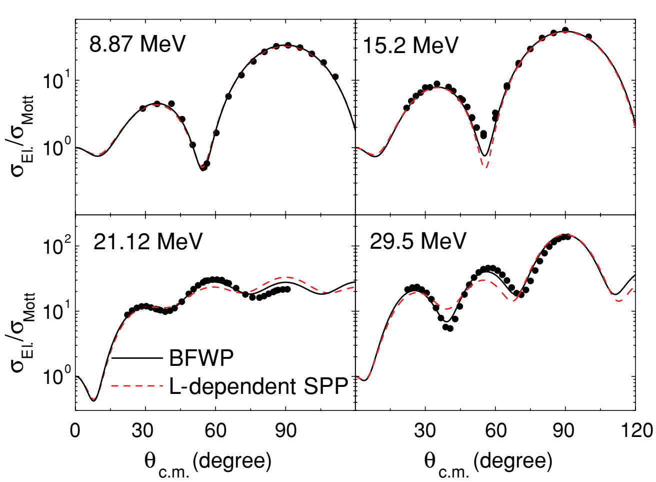

FIG. 7. (Color online) The same as Fig. 6, for $E_{\mathrm{Lab}} = 8.87$, 15.2, 21.12, and 29.5 MeV (data from Refs. [37,39,40]).

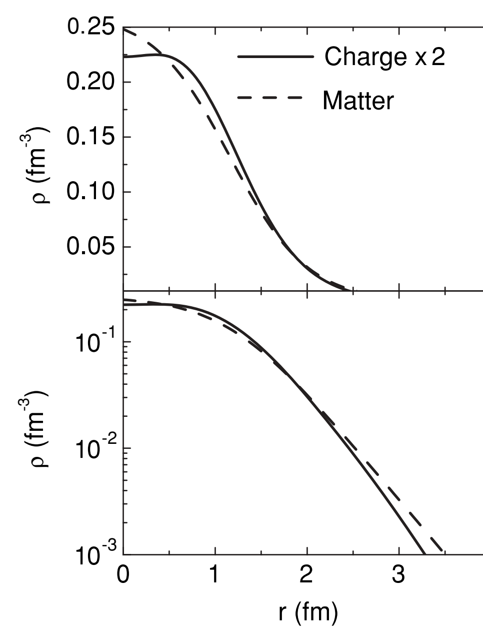

FIG. 8. Comparison between the best-fit matter (dashed lines) and charge (solid lines) distributions. Because of the different normalizations, in the figure the charge distribution is multiplied by two. The data are shown in linear (top) and logarithmic (bottom) scales.

This sort of effect is usually neglected at low energies because of the corresponding low velocity. This is, in fact, the case when considering heavy-ion systems where the scattering is sensitive only to the surface region of the interaction. As already commented, in the present case the relative velocity can reach significant values at smaller separations. Note that $v \approx 0.34\,c$ represents a factor of contraction of $\sqrt{1 - v^2/c^2} \approx 0.94$. If this contraction is applied to the α density, because of the folding procedure the corresponding potential would also be slightly deformed and, therefore, a weak L dependence should be expected. Nevertheless, it is not simple to introduce this effect within the context of the Schrödinger equation. Thus, in this work we have not investigated quantitatively the possible effects of the contraction on the cross sections.

Finally, for the purpose of comparison, we have also calculated volume integrals and corresponding root-mean-square radii ($R_{\rm rms}$) for the different α-α interactions. We obtained $J_R = 414$ MeV fm^3 and $R_{\rm rms} = 2.61$ fm for the BFWP, $J_R = 405$ MeV fm^3 and $R_{\rm rms} = 2.48$ fm for the SPP in the context of the same shape for matter and charge distributions and with $N = 1.08$, and $J_R = 427$ MeV fm^3 and $R_{\rm rms} = 2.66$ fm for the SPP with the Fermi distribution and $N = 1.1144$. As expected, because of the similarities among these potentials, the three different models provide values for J_R and $R_{\rm rms}$ that agree within about 5%.

V. EFFECT OF THE RENORMALIZATION OF THE SPP ON THE RESULTS FOR HEAVY-ION SYSTEMS

The description of the $\alpha + \alpha$ elastic scattering in the context of the SPP requires a renormalization of the V_0 value by about 10%. On the other hand, the standard SPP ($N = 1$) was quite successful in data analyses of heavy-ion systems. This discrepancy is unsatisfactory if we wish to obtain a general model for light and heavy ions. In this section, we study the effect of the V_0 renormalization on the results for heavy-ion systems. We show that this effect is not very significant if we introduce a small modification in the standard diffuseness value assumed in the systematics of the matter distributions of heavy ions.

The standard V_0 and density parameters of the SPP were established in Ref. [2]. The method employed was the adjustment of the phenomenological strength of the real part of the optical potential obtained from data analyses for many systems and in a large energy range. In that work, the Fermi distribution [Eq. (4) in the present work] was assumed to describe the nuclear densities. The R_0 and a parameters were obtained from theoretical calculations and also from experimental charge distributions. Within this systematics, it was found that the average behavior of the nuclear radii can be well described by $R_0 = 1.31\,A^{1/3} - 0.84$ fm. An average diffuseness for the matter distributions of $a = 0.54$ fm resulted from the theoretical calculations. However, because of a small difference found between the theoretical and experimental charge diffuseness values, in Ref. [2] it was assumed that a slightly larger value should also be adopted for the matter distributions: $a = 0.56$ fm. In the present work, we have performed new calculations that show that a good description of the phenomenological strengths is also obtained with V_0 increased by about 10% and a decreased by about 3%. Figure 9 (bottom) shows the experimental and theoretical (solid line) reduced strengths as a function of the distance between the surfaces of the nuclei as obtained in Ref. [2], that is, with $V_0 = -456$ MeV fm^3 and $a = 0.56$ fm (see Ref. [2] for the definition of the reduced potential strength). Figure 9 (top) shows the present results with $V_0 = -500$ MeV fm^3 and $a = 0.545$ fm. No significant difference is obtained with the present parameters in comparison with those reported in Ref. [2]. This is a clear indication that the results for systems involving heavy ions can be described with similar accuracy by the two sets of parameters.

VI. CONCLUSION

Because of the complicated structure of heavy nuclei, heavy-ion data analyses always involve a certain degree of modeling and simplification in theoretical calculations. On the other hand, because of the complete lack of open reaction channels, α scattering at low energies can be treated on much more fundamental grounds. For this system, owing to the vanishing imaginary part of the optical potential, the cross-section data analysis is quite sensitive to the real part of the interaction, even at quite internal distances. Thus, the present $\alpha + \alpha$ data analyses represent an important test of the SPP, which was very successful in describing heavy-ion reactions. We verified that to reproduce the $\alpha + \alpha$ data in the context of the SPP, it

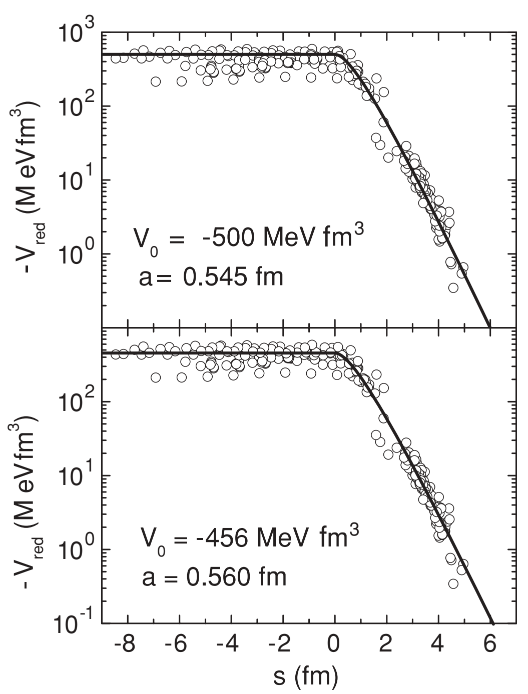

FIG. 9. Experimental and theoretical reduced potentials as a function of the distance between the surface of the nuclei. (Bottom) Calculations performed considering the original V_0 and a parameter values of Ref. [2]. (Top) Present calculations with $V_0 = -500$ MeV fm^3 and $a = 0.545$ fm. See Ref. [2] to obtain the definition of the reduced potential strength.

was necessary to introduce a renormalization of about 10% in the V_0 value. As we demonstrated, to make this new V_0 value compatible with the previous results of heavy-ion systems, a small reduction of the average diffuseness value assumed for the heavy-ion matter distributions to $a \approx 0.545$ fm is required.

The $\alpha + \alpha$ elastic scattering data are well described within two different approaches. In one of them, there is no L dependence in the interaction but it was necessary to assume that the α matter and charge distributions have different shapes. In the other, the matter distribution is simply twice that of the charge distribution, but a weak L dependence in the interaction is necessary to describe the data. This angular momentum dependence could be related to the effects of the relativistic contraction of space because, even at low bombarding energies, the relative velocity between the α particles can reach significant values at smaller separations. Although this hypothesis seems reasonable from a qualitative point of view, it should be tested quantitatively in future works. The present work represents a step in the direction of extending the SPP model to systems involving light nuclei.

ACKNOWLEDGMENTS

This work was partially supported by the Fundação de Amparo à Pesquisa do Estado de São Paulo (FAPESP) and the Conselho Nacional de Desenvolvimento Científico e Tecnológico (CNPq).

[1] M. E. Brandan and G. R. Satchler, Phys. Rep. **285**, 143 (1997).
[2] L. C. Chamon, B. V. Carlson, L. R. Gasques, D. Pereira, C. De Conti, M. A. G. Alvarez, M. S. Hussein, M. A. Candido Ribeiro, E. S. Rossi Jr., and C. P. Silva, Phys. Rev. C **66**, 014610 (2002).
[3] L. C. Chamon, D. Pereira, M. S. Hussein, M. A. Candido Ribeiro, and D. Galetti, Phys. Rev. Lett. **79**, 5218 (1997).
[4] M. A. G. Alvarez, L. C. Chamon, M. S. Hussein, D. Pereira, L. R. Gasques, E. S. Rossi Jr., and C. P. Silva, Nucl. Phys. A **723**, 93 (2003).
[5] S. Mukherjee, B. K. Nayak, D. S. Monteiro, J. Lubian, P. R. S. Gomes, S. Appannababu, R. K. Choudhary, Phys. Rev. C **80**, 014607 (2009).
[6] D. S. Monteiro *et al.*, Phys. Rev. C **79**, 014601 (2009).
[7] A. Barioni *et al.*, Phys. Rev. C **80**, 034617 (2009).
[8] J. P. Fernandez-Garcia, M. Rodriguez-Gallardo, M. A. G. Alvarez, and A. M. Moro, Nucl. Phys. A **840**, 19 (2010).
[9] G. P. A. Nobre, L. C. Chamon, L. R. Gasques, B. V. Carlson, and I. J. Thompson, Phys. Rev. C **75**, 044606 (2007).
[10] G. P. A. Nobre, C. P. Silva, L. C. Chamon, and B. V. Carlson, Phys. Rev. C **76**, 024605 (2007).
[11] L. F. Canto, P. R. S. Gomes, J. Lubian, L. C. Chamon, and E. Crema, Nucl. Phys. A **821**, 51 (2009).
[12] P. R. S. Gomes, J. Lubian, and L. F. Canto, Phys. Rev. C **79**, 027606 (2009).
[13] D. Pereira *et al.*, Phys. Rev. C **74**, 034608 (2006).
[14] L. C. Chamon, D. Pereira, and M. S. Hussein, Phys. Rev. C **58**, 576 (1998).
[15] M. Avrigeanu, A. C. Obreja, F. L. Roman, V. Avrigeanu, and W. von Oertzen, At. Data Nucl. Data Tables **95**, 501 (2009).
[16] M. Ermer, H. Clement, G. Frank, P. Grabmayr, H. Heberle, and G. J. Wagner, Phys. Lett. B **224**, 40 (1989).
[17] M. Avrigeanu, W. von Oertzen, A. J. M. Plompen, and V. Avrigeanu, Nucl. Phys. A **723**, 104 (2003).
[18] P. Demetriou, C. Grama, and S. Goriely, Nucl. Phys. A **707**, 253 (2002).
[19] F. Michel and R. Wanderpoorten, Phys. Rev. C **16**, 142 (1977).
[20] L. R. Gasques *et al.*, Phys. Rev. C **67**, 024602 (2003).
[21] K. Langanke and C. Rolfs, Z. Phys. A **324**, 307 (1986).
[22] K. Langanke and C. Rolfs, Phys. Rev. C **33**, 790 (1986).
[23] P. Mohr *et al.*, Z. Phys. A **349**, 339 (1994).
[24] V. M. Datar, S. Kumar, D. R. Chakrabarty, V. Nanal, E. T. Mirgule, A. Mitra, and H. H. Oza, Phys. Rev. Lett. **94**, 122502 (2005).
[25] S. A. Afzal, A. A. Z. Ahmad, and S. Ali, Rev. Mod. Phys. **41**, 247 (1969).
[26] H. Friedrich, Phys. Rep. **74**, 209 (1981).
[27] B. Buck, H. Friedrich, and C. Wheatley, Nucl. Phys. A **275**, 246 (1977).
[28] D. Galetti, S. S. Mizrahi, L. C. Chamon, D. Pereira, M. S. Hussein, and M. A. Candido Ribeiro, Phys. Rev. C **58**, 1627 (1998).
[29] M. A. Candido Ribeiro, L. C. Chamon, D. Pereira, M. S. Hussein, and D. Galetti, Phys. Rev. Lett. **78**, 3270 (1997).
[30] H. De Vries, C. W. De Jager, and C. De Vries, At. Data Nucl. Data Tables **36**, 495 (1987).
[31] U. Atzrott, P. Mohr, H. Abele, C. Hillenmayer, and G. Staudt, Phys. Rev. C **53**, 1336 (1996).
[32] L. C. Chamon and M. A. G. Alvarez, Phys. Rev. C **72**, 014603 (2005).
[33] V. I. Kukulin, V. G. Neudatchin, and Yu F. Smirnov, Nucl. Phys. A **245**, 429 (1975).
[34] D. Baye, P. Descouvemont, and M. Kruglanski, Nucl. Phys. A **550**, 250 (1992).
[35] J. L. Russel Jr., G. C. Phillips, and C. W. Reich, Phys. Rev. **104**, 135 (1956).
[36] N. P. Heydenburg and G. M. Temmer, Phys. Rev. **104**, 123 (1956).
[37] R. Nilson, R. O. Kerman, G. R. Brigs, and W. K. Jentschke, Phys. Rev. **104**, 1673 (1956).
[38] R. Nilson, W. K. Jentschke, G. R. Brigs, R. O. Kerman, and J. N. Snyder, Phys. Rev. **109**, 850 (1958).
[39] T. A. Tombrello and L. S. Senhouse, Phys. Rev. **129**, 2252 (1963).
[40] W. S. Chien and R. E. Brown, Phys. Rev. C **10**, 1767 (1974).